ARTICLE OPEN

Check for updates

Psychedelic compounds directly excite 5-HT_{2A} layer V medial prefrontal cortex neurons through 5-HT_{2A} Gq activation

Gavin P. Schmitz[1], Yi-Ting Chiu[1], Mia L. Foglesong[1], Sarah N. Magee[1], Martin MacKinnon[2,3], Gabriele M. König[4], Evi Kostenis[5], Li-Ming Hsu[2,3,6], Yen-Yu I. Shih[2,3,7], Bryan L. Roth[1] and Melissa A. Herman[1]✉

© The Author(s) 2025

Psilocybin, and its active metabolite psilocin, have seen renewed interest due to studies suggesting potential therapeutic utility. 5-Hydroxytryptamine2A receptors (5-HT_{2A}Rs) are primary mediators of the psychoactive effects of psychedelics in animals and humans, but the underlying neurobiological mechanisms remain poorly understood. Functional magnetic resonance imaging identified significant psilocin-induced increases in medial prefrontal cortex (mPFC) activity, a site of enriched 5-HT_{2A}R expression. We identified a population of 5-HT_{2A}R neurons in the prelimbic/anterior cingulate mPFC. Psilocin and the 5-HT_{2A}R-selective compound 25-CN-NBOH increased excitability, and stimulated firing across a range of current injections in these neurons that was both 5-HT_{2A}R and $G\alpha_q$ dependent. Similar effects were observed with a novel, non-hallucinogenic psychedelic compound. These findings provide valuable insight into the specific role of 5-HT_{2A}R-containing neurons in psychedelic-associated plasticity in mPFC regions that are likely implicated in the clinical effects of psychedelics and further identify membrane-bound 5-HT_{2A}Rs and subsequent intracellular $G\alpha_q$ signaling as therapeutic targets.

Translational Psychiatry (2025)15:381 ; https://doi.org/10.1038/s41398-025-03611-0

INTRODUCTION

Psychedelic compounds act at 5-hydroxytryptamine 5-HT_{2A} receptors [1, 2] and are being explored as potential therapeutics for neuropsychiatric disorders [3]. Psilocybin, the prodrug to the active metabolite psilocin, was granted breakthrough status by the FDA for rapid and enduring effects in treatment-resistant depression and anxiety [4–7]. Psychedelics act at serotonin and other biogenic amine receptors [8–12] and 5-HT_{2A} agonism has been shown to mediate purported hallucinogenic effects in animals [13–15] and humans [16–19]. 5-HT_{2A} receptors signal through $G\alpha_q$ downstream effector systems [2, 20, 21], recruit β-arrestin (βArr) in vitro [22], and 5-HT_{2A} complexes with βArr1 and βArr2 in vivo [23]. There is current interest in creating biased compounds to preferentially activate desired pathways downstream of 5-HT_{2A} [24–27], however, the signaling pathways of psychedelics in therapeutically-relevant brain regions remain unclear.

In humans, the psychedelic effects of psilocin correlate with 5-HT_{2A} occupancy in the prefrontal cortex (PFC) [28]. Psilocybin increases excitatory neurotransmission in medial PFC (mPFC) neurons and produces long-lasting changes in dendritic architecture [29]. Despite significant 5-HT_{2A} expression in the mPFC, the actions of psychedelics on 5-HT_{2A} mPFC neurons remain largely unexamined; however, one recent study found cell-type specific effects of psilocybin where increased excitability and persistent behavioral effects were mediated by subcortical projection pyramidal tract mPFC cells that demonstrated increased synaptic calcium transients and firing rates acutely after administration [30]. Patients with treatment-resistant depression report that psilocin increases ability to modulate self-focus, reduces negative emotional processing, and strengthens social functioning [31, 32], processes governed by mPFC in maintaining a sense of self [33]. The goal of the present study was to investigate the actions of psilocin in mPFC 5-HT_{2A} neurons and determine the receptor pharmacology and intracellular signaling pathways involved to uncover the neurobiological mechanisms that may be implicated in the therapeutic actions of psilocybin and other psychedelics.

MATERIALS AND METHODS

Animals

Experiments were conducted in adult (>P60, 19–30 g) male and female C57BL6/J or 5-HT_{2A}R-eGFP-CreERT2xAi9 mice that express 5-HT_{2A} tagged with GFP at the C-terminus with tamoxifen-induced cre-recombination. Tamoxifen (100 mg/kg, i.p.) was administered once/day for 4 d in mice ≥P35, to ensure adult receptor expression. Mice were bred in-house and maintained with ad libitum access to food, water, and environmental enrichment.

Ethics approval

All experimental parameters and procedures are in accordance with NIH Guidelines and approved by the UNC Institutional Animal Care and Use

[1]Department of Pharmacology, University of North Carolina at Chapel Hill School of Medicine, Chapel Hill, NC, USA. [2]Center for Animal MRI, University of North Carolina at Chapel Hill School of Medicine, Chapel Hill, NC, USA. [3]Biomedical Research Imaging Center, University of North Carolina at Chapel Hill School of Medicine, Chapel Hill, NC, USA. [4]Institute of Pharmaceutical Biology, University of Bonn, Bonn, Germany. [5]Molecular, Cellular and Pharmacobiology Section, Institute of Pharmaceutical Biology, University of Bonn, Bonn, Germany. [6]Departmental of Radiology, University of North Carolina at Chapel Hill School of Medicine, Chapel Hill, NC, USA. [7]Department of Neurology, University of North Carolina at Chapel Hill School of Medicine, Chapel Hill, NC, USA. ✉email: melissa_herman@unc.edu

Received: 15 August 2024 Revised: 1 August 2025 Accepted: 1 September 2025
Published online: 06 October 2025

Committee [NIH/PHS Animal Welfare Assurance Number: D16-00256 (A3410-01].

Functional magnetic resonance imaging (fMRI)

Mice were anesthetized with isoflurane (2–3% induction, 0.5–0.75% maintenance) while preserving physiological homeostasis. The cradle was pushed into MRI bore, and dexmedetomidine (0.0125 ug/kg, i.p., initial bolus; 0.05 ug/kg/hr, continuous infusion) was administered. Imaging was performed on a Bruker BioSpec 9.4-Tesla, 30 cm bore system with ParaVision 360.1.0 on an AVANCE NEO console, and an RRI BFG 240/120, 1000 mT/m gradient insert (Resonance Research Inc.) paired with an IECO GPA-400-350 gradient amplifier (International Electric Company). A homemade surface coil (1 cm I.D.) with a miniature circuit board served as a radio frequency transceiver. Magnetic field homogeneity was optimized first by global shimming, followed by local second-order shims using a Scan Shim protocol. fMRI data were acquired using a ZTE-like imaging sequence: spoke-TR (repetition time) = 0.6 ms, flip angle = 3°, initial matrix size = 16 × 16 × 16, initial FOV (field of view) = 6.4 × 6.4 × 6.4 mm, nominal acquisition bandwidth 17 kHz (nominal sampling interval 60 µs), spoke-oversampling factor = 8 (i.e., digitizing bandwidth = 136 kHz), reconstructed matrix size = 48 × 48 × 48, reconstructed FOV = 19.2 × 19.2 × 19.2 mm, total number of spokes per volume = 3310, RF pulse-duration = 4 µs, T-R switch deadtime = 4.75 µs, and dummy scan duration = ~10 s.

Subjects were scanned for 90 min in three periods: Baseline (15 min), Vehicle (15 min: 5 kg/ml, s.c. 2% acetic acid in saline), and Drug Period (2 mg/kg, s.c. psilocin continued for remainder of scanning). Body temperature was maintained at 37 ± 0.5 °C, respiration was monitored through a pneumatic pillow (Respiration/EEG Monitor, SA Instruments) and maintained between 90–110 breaths/min. A circulating water bath (Haake S13, Thermo Scientific) heats the MRI mouse cradle.

Brain images were isolated with our U-Net deep-learning tool specifically designed for skull stripping [34, 35]. Images were spatially normalized to fit a ZTE template, and motion correction and smoothing processes were executed using AFNI software [36]. For smoothing, a Gaussian kernel with a full width at half maximum (FWHM) of 0.8 mm was utilized. We then estimated the averaged time series in three selected mPFC regions: prelimbic (PrL), infralimbic (IL), and anterior cingulate cortex (ACC, Fig. 1A) according to Allen brain atlas [37]. For each time series, effects of motion were regressed out. To account for linear drift, the linear trend was identified within the vehicle and subsequently regressed out across the entire time series. This detrending process involved fitting a linear model to a specific set of data points within the vehicle and then subtracting this trend line from the original time series. Finally, the entire time series was normalized using the mean and standard deviation computed from the baseline period. A linear mixed-effects model (LME) [38, 39] was used to analyze the interaction effects of brain regions (IL, ACC, PrL) and experimental groups (Experiment vs. Control) on fMRI responses. The model included brain regions (IL, ACC, PrL) as a fixed effect, group (Experiment vs. Control) as a fixed effect, and subject as a random effect to account for individual variability.

Electrophysiological recording

Brains were removed and placed in ice-cold (in mM): sucrose 206.0; KCl 2.5; $CaCl_2$ 0.5; $MgCl_2$ 7.0; NaH_2PO_4 1.2; $NaHCO_3$ 26; glucose 5.0; HEPES 5. Coronal sections (300µm) were prepared on a vibrating microtome (Leica VT1000S) and incubated in 95% O_2/5% CO_2 aCSF (in mM): NaCl 130; KCl 3.5; Glucose 10; NaHCO3 24; MgSO4-7H2O 1.5; NaH2PO4-H2O 1.26; CaCl 2.0 for 30 min at 37 °C and 30 min at room temperature (RT). Pipettes (4-6 MΩ) were filled with internal solution (in mM: KCl 145; EGTA 5; $MgCl_2$ 5; HEPES 10; Na-ATP 2; Na-GTP 0.2 or Kgluconate 145; EGTA 5; $MgCl_2$ 5; HEPES 10; Na-ATP 2; Na-GTP 0.2). Recordings were performed at RT with a Multiclamp 700B amplifier (Molecular Devices) at a sampling rate of 10,000 Hz, low-pass filtered at 2-5 kHz, digitized (Digidata 1550B; Molecular Devices) and stored using pClamp 10 software (Molecular Devices). Series resistance was monitored with 10 mV hyperpolarizing pulses; cells with $R_a > 20$ MΩ were excluded from analysis. 5-HT_{2A} neurons were identified using <2 s episodic fluorescent illumination. Current-clamp recordings measured firing and voltage-clamp recordings ($V_{hold} = -70$ mV) of excitatory and inhibitory postsynaptic currents (EPSCs/IPSCs) were performed using 6,7-dinitroquinoxaline-2,3-dione (DNQX, 20 µM), DL-2-amino-5-phosphonovalerate (AP-5, 50 µM), and CGP55845 (1 µM) for IPSCs and gabazine (SR-95531, 20 µM) and CGP55845 (1 µM) for EPSCs. Miniature inhibitory and excitatory synaptic currents (mIPSCs/mEPSCs) were measured using tetrodotoxin (1 µM). Drugs were focally applied by a y-tube filament positioned in close proximity to the recorded cell with vehicle (aCSF) solution exchange performed prior to drug application (5–10 min). Drugs were made fresh on the day of recording, dissolved to experimental concentrations in aCSF, and stored in closed conical tubes except while being applied during experimental recording. Series resistance was continuously monitored throughout recording and cells with >25% change in access resistance were excluded from data analysis. Firing frequency was quantified by Clampfit (Molecular Devices) and IPSCs/EPSCs were analyzed using MiniAnalysis (Synaptosoft) using an analysis period with >60 events. Experimental drugs were only applied once per slice to avoid confounds of repeated application.

Cell culture

HEK293T cells were authenticated by and obtained from ATCC, and mycoplasma testing was performed upon arrival by standard laboratory practices. Cells were maintained, passaged, and transfected in Dulbecco's Modified Eagle's Medium containing 10% fetal bovine serum (FBS), 100 Units/mL penicillin, and 100 µg/mL streptomycin in a humidified atmosphere at 37 °C and 5% CO2. After transfection, cells were plated in DMEM containing 1% dialyzed FBS, 100 Units/mL penicillin, and 100 µg/mL streptomycin for BRET assays.

BRET2 assays

Cells were plated in six-well dishes at a density of 700,000–800,000 cells/well. Cells were transfected 2–4 hr later, using a 1:1:1:1 DNA ratio of receptor:Gα-RLuc8:Gβ:Gγ-GFP2 (100 ng/construct). Transit 2020 was used to complex the DNA at a ratio of 3 µL Transit/µg DNA, in OptiMEM at a concentration of 10 ng DNA/µL OptiMEM. Next day, cells were harvested and plated in poly-D-lysine-coated white, clear bottom 96-well assay plates at a density of 30,000–50,000 cells/well.

One day after plating, white backings were applied to the plate bottoms, and growth medium was carefully aspirated and replaced with 50 µL assay buffer (1 × HBSS + 20 mM HEPES, pH 7.4) containing fresh 50 µM coelenterazine 400a. After 5 min equilibration, cells were treated with 50 µL of drug (2X) for an additional 5 min. Plates were read in a Pherastar FSX microplate reader with 395 nm (RLuc8-coelenterazine 400a) and 510 nm (GFP2) emission filters, at 1 s/well integration times. BRET2 ratios were computed as the ratio of the GFP2 emission to RLuc8 emission. Results are from ≥3 independent experiments, each performed in duplicate. Data were normalized to 5-HT stimulation and analyzed using nonlinear regression "log(agonist) vs. response".

Drugs

Drugs were purchased as follows: psilocin (Cayman chemical), RS102221 (Tocris Bioscience), and M100907 (Sigma-Aldrich). FR900359 was obtained from Evi Kostenis [40]. Stock solutions were prepared in ultra-pure water or DMSO, stored at −20 °C and diluted to experimental concentrations in aCSF.

Statistical analysis

Experimental subjects were randomly assigned to treatment groups and sample sizes were calculated based on the minimum numbers required to see statistically significant changes as determined by previous studies. Data analysis and visualization were completed with Prism 9 (GraphPad) by investigators unblinded to treatment condition. Membrane characteristics were represented as mean ± SEM and compared via two-way ANOVA (sex x response). sIPSC/sEPSCs were analyzed and visually confirmed using threshold-based detection software (MiniAnalysis, Synaptosoft). Data were analyzed by paired or unpaired t-test, and normalized data were analyzed by one-sample t-test, where appropriate. Concentration-response curves were fit to a three-parameter logistic equation in Prism 9 (Graphpad). BRET2 concentration-response curves were analyzed as either raw net BRET2 (fit Emax-fit Baseline) or by normalizing to a reference agonist for each experiment. Efficacy (Emax) calculations were performed as previously described [41]: stimulus-response amplitudes (net BRET2) were normalized to the maximal responding agonist (maximal system response). EC50 and Emax values were estimated from the simultaneous fitting of all biological replicates.

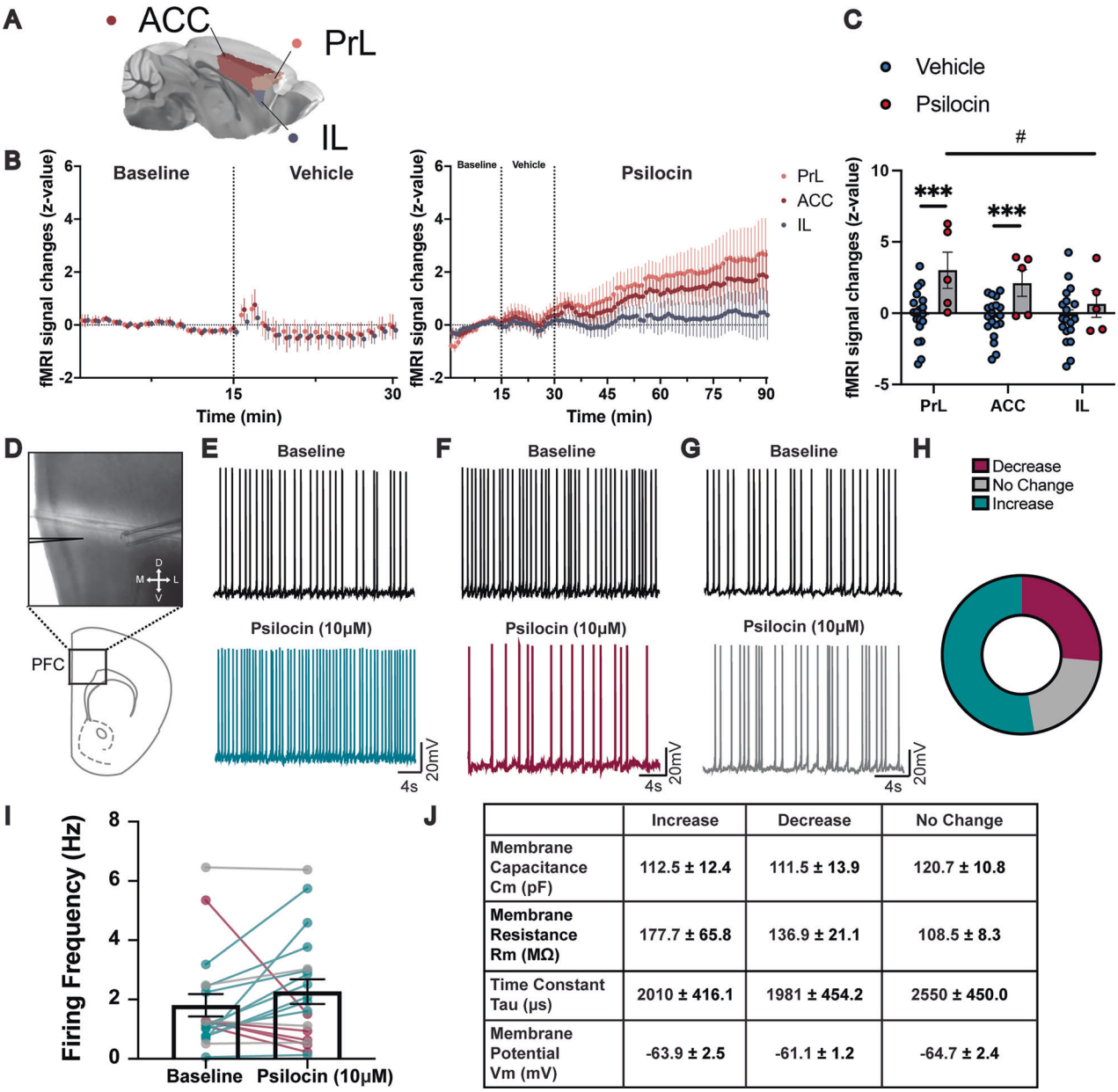

	Increase	Decrease	No Change
Membrane Capacitance Cm (pF)	112.5 ± 12.4	111.5 ± 13.9	120.7 ± 10.8
Membrane Resistance Rm (MΩ)	177.7 ± 65.8	136.9 ± 21.1	108.5 ± 8.3
Time Constant Tau (μs)	2010 ± 416.1	1981 ± 454.2	2550 ± 450.0
Membrane Potential Vm (mV)	-63.9 ± 2.5	-61.1 ± 1.2	-64.7 ± 2.4

Fig. 1 Psilocin effects in medial prefrontal cortex and on layer 5 pyramidal neurons from C57B6/J mice. A A representative 3D plot of the three selected anatomical regions within the prefrontal cortex: prelimbic (PrL), infralimbic (IL), and anterior cingulate cortex (ACC). **B** The fMRI signal normalized to the baseline (Error bars represent the standard error) in experiment and control groups. **C** Averaged fMRI signal changes in PrL, ACC, and IL during the psilocin period in the experimental group and the vehicle period in the control group (*F*-value = 8.10, $p < 0.001$). PrL exhibited a trend toward higher fMRI activity compared to IL ($\beta = 2.36$, $^{\#}p = 0.059$). Additionally, fMRI responses in ACC and PrL were significantly elevated in the experimental group relative to the control group (ACC: $\beta = 3.13$, $^{***}p < 0.005$; PrL: $\beta = 2.43$, $^{***}p < 0.005$). **D** Representative PFC Layer 5 pyramidal neuron location within slice. Representative recordings of neuronal firing after psilocin (10 μM) showing increase (**E**), decrease (**F**), and no change (**G**). **H** Graphical depiction of differential neuronal responses to psilocin (10 μM). (**I**) Averaged psilocin effects on firing in L5P (mean ± SEM, n = 19). **J** Membrane characteristics of layer V pyramidal neurons (mean ± SEM).

RESULTS

Psilocin effects on layer 5 pyramidal neurons from C57B6/J mice

To examine global effects of psilocin, we performed fMRI in C57BL6/J mice following systemic administration of vehicle or psilocin (2 mg/kg, s.c.), an active dose that has been shown to produce reliable increases in head twitch responding in mice [42, 43]. We delineated three mPFC regions: the prelimbic (PrL), infralimbic (IL), and anterior cingulate cortex (ACC; Fig. 1A) and extracted the fMRI signal. The time series demonstrate increases in activity in the ACC, PrL, and IL after psilocin, with the greatest change in the PrL (Fig. 1B). The LME model assessing the effects of brain regions (PrL, ACC, IL) and experimental groups (Experiment vs. Control) on fMRI responses revealed a significant interaction between group and brain regions was observed (*F*-value = 8.10, $p < 0.001$) (Fig. 1C), indicating that the effect of group on fMRI responses varied by brain region. To further explore these regional differences, additional pairwise LME comparisons were conducted within the experimental group. A trend toward higher activity was observed in PrL compared to IL ($\beta = 2.36$, $p = 0.059$). However, no significant differences were found in the comparisons of PrL vs. ACC and ACC vs. IL within the experimental group. Further

between-group comparisons within each brain region revealed significant effects. The experimental group exhibited significantly higher responses compared to the control group in both PrL ($\beta = 3.13$, $p < 0.005$) and ACC ($\beta = 2.43$, $p < 0.005$). However, no significant difference between groups was observed in IL. These findings suggest that while ACC and PrL exhibited increased activity during psilocybin administration in the experimental group, this enhancement was not present in the control group, highlighting a group-dependent modulation of fMRI responses across brain regions.

To examine psilocin's cellular effects, we performed electrophysiological recordings in PrL/ACC mPFC neurons (Fig. 1D). Layer 5 pyramidal neurons were identified based on morphology and membrane characteristics. Current (<120pA) was injected to bring neurons to a stable firing rate and held constant for the duration of the experiment. Psilocin (10 μM) produced variable effects on layer 5 pyramidal neurons in the PrL/ACC mPFC (Fig. 1E-I). Psilocin increased firing (>120% change) in most neurons (n = 10 neurons/N = 6 mice; Figs. 1E, 1H), decreased firing (<80% change) in ~30% of neurons (n = 5 neurons/N = 4 mice; Fig. 1F, 1H), and produced no change in firing (80–120% change) in the remaining neurons (n = 4 neurons/N = 4 mice; Fig. 1G, 1H). There were no significant differences in membrane properties between groups (Fig. 1J).

Psilocin effects on excitability and synaptic transmission in 5-HT$_{2A}$ neurons

To examine the effects of psilocin on 5-HT$_{2A}$ mPFC neurons, we utilized a 5-HT$_{2A}$-tdTomato-reporter mouse with cre-dependent expression of 5-HT$_{2A}$. We observed tdTomato expression throughout PrL/ACC mPFC (Fig. 2A). 5-HT$_{2A}$ neurons were identified based on morphology and tdTomato expression (Fig. 2B). Initial recordings were performed in tdTomato non-expressing 5-HT$_{2A}$ negative as well as TdTomato expressing 5-HT$_{2A}$ neurons, however consistent with unspecified neurons (Figs. 1E-H), 5-HT$_{2A}$ negative neurons had variable responses so all subsequent experiments focused solely on 5-HT$_{2A}$ neurons. Current was injected to achieve stable spontaneous firing and held constant for the duration of continuous firing recordings. Recordings were performed across a range of firing frequencies (< 1-6 Hz) including more elevated (4-6 Hz) and lower frequencies (<1-2 Hz) to examine any differences in drug effect at different baseline firing rates. Focal application of psilocin (10μM) increased firing in 5-HT$_{2A}$ neurons (n = 13 cells/N = 10 mice, *paired* t-test **p < 0.01; Fig. 2C, D) to ~200% of baseline (n = 13 cells/N = 10 mice, one-sample t-test ***p < 0.001; Fig. 2E). Increased firing was observed in males and females with moderately larger effects in males (Figure S1A–C). To assess intrinsic excitability, we performed episodic current-clamp recordings in 5-HT$_{2A}$ neurons with increasing current steps and measured current-evoked firing (number of action potentials at each current injection), rheobase (current injection at which the first action potential was elicited), and threshold to fire (voltage at which the first action potential was elicited). Psilocin (10 μM) increased firing in 5-HT$_{2A}$ neurons at 20, 60, and 100pA (n = 10–25 cells/N = 12 mice, *paired* t-test *p < 0.05 - **p < 0.01; Fig. 2F). Psilocin also reduced the threshold to fire (n = 25 cells/N=12mice, *paired* t-test *p < 0.05; Fig. 2G) and rheobase (current required to elicit an action potential), (n = 25 cells/N = 12 mice, *paired* t-test ***p < 0.001; Fig. 2H).

We performed voltage-clamp recordings measuring glutamatergic transmission in 5-HT$_{2A}$ neurons. Psilocin (10μM) produced no changes in spontaneous excitatory post-synaptic current (sEPSC) frequency in raw (n = 12 cells/N = 8 mice, Fig. 2I, J) or normalized values (Fig. 2K) or in raw (Fig. 2L) or normalized sEPSC amplitude (Fig. 2M). Psilocin (10 μM) also produced no changes in mEPSC frequency or amplitude (Figure S2A–E). We performed voltage-clamp recordings measuring inhibitory transmission in 5-HT$_{2A}$ neurons. Psilocin (10 μM) produced no changes in spontaneous inhibitory post-synaptic current (sIPSC) frequency or amplitude (Figure S3A–E).

5-HT2A-selective agonist NBOH-2C-CN effects on excitability and synaptic transmission in 5-HT2A neurons

We also performed recordings using the selective 5-HT$_{2A}$ agonist NBOH-2C-CN. To guide dose selection, we conducted a TRUPATH Gα_q dissociation experiment at the mouse 5-HT$_{2A}$R [44]. The concentration response curve showed that NBOH-2C-CN had increased potency compared to Psilocin (46 nM vs 7 nM, F-test **p < 0.01; Fig. 3A) so 200 nM was selected to reflect potency differences and minimize off-target effects. NBOH-2C-CN (200 nM) increased firing in 5-HT$_{2A}$ neurons (n = 8 cells/N = 4 mice, *paired* t-test *p < 0.05; Fig. 3B,C) to ~200% of baseline (n = 8 cells/N = 4 mice, one-sample t-test **p < 0.01; Fig. 3D). More pronounced increases were observed in males compared to females (Fig. S1D, E) with no differences overall (Fig. S1F). NBOH-2C-CN (200 nM) did not alter current-evoked firing in 5-HT$_{2A}$ neurons at 20, 60, and 100 pA (n = 10–12 cells/N = 8 mice; Fig. 3E), but significantly reduced threshold to fire (n = 11 cells/N = 7 mice, *paired* t-test *p < 0.05; Fig. 3F) and rheobase (n = 11 cells/N = 7 mice, *paired* t-test *p < 0.05; Fig. 3G).

NBOH-2C-CN (200 nM) produced no change in 5-HT$_{2A}$ neuron sEPSC frequency in raw (n = 7 cells/N = 5 mice, Fig. 3H, I) or normalized values (Fig. 3J). NBOH-2C-CN produced no changes in raw (Fig. 3K) or normalized sEPSC amplitude (Fig. 3L). NBOH-2C-CN also produced no change in mEPSC frequency or amplitude (Fig. S2F-J) and no changes in sIPSC frequency or amplitude (Figure S3F-J).

5-HT$_{2A}$ receptor involvement in the effects of psilocin and NBOH-2C-CN on 5-HT$_{2A}$ neurons

To examine the role of 5-HT$_{2A}$ receptors 5-HT$_{2A}$ neuron activity and in the effects of psilocin and NBOH-2C-CN, we performed current-clamp recordings with the 5-HT$_{2A}$-specific antagonist M100907. M100907 (200 nM) decreased 5-HT$_{2A}$ neuron firing (n = 10 cells/N = 6 mice, *paired* t-test *p < 0.05; Fig. 4A, B) to ~40% of baseline (n = 10 cells/N = 6 mice, one-sample t-test *p < 0.05; Fig. 4C). Subsequent application of psilocin (10 μM) with M100907 (200 nM) had no effect on firing (n = 10 cells/N = 6 mice, Fig. 4A, D) or normalized firing (n = 10 cells/N = 6 mice, Fig. 4E). In separate recordings, M100907 (200 nM) decreased firing in 5-HT$_{2A}$ neurons (n = 9 cells/N = 5 mice, *paired* t-test *p < 0.05; Fig. 4F, G) to ~35% of baseline (n = 9 cells/N = 5 mice, one-sample t-test *p < 0.05; Fig. 4H). Subsequent NBOH-2C-CN (200 nM) application with M100907 (200 nM) did not alter firing (n = 11 cells/N = 5 mice, Fig. 4F, I). When frequencies were normalized to baseline, no effect on firing frequency was observed (n = 10 cells/N = 5 mice, Fig. 4J). To examine whether these actions could be applied in drug discovery, we examined the effects of the novel non-hallucinogenic, therapeutic 5-HT$_{2A}$R agonist R-70 [25]. R-70 (10 μM) significantly increased firing consistent with the effects of psilocin and NBOH-2C-CN (Figure S4A, B). These effects were also blocked by prior administration of the 5-HT$_{2A}$-specific antagonist M100907 (Figure S4C–F).

5-HT$_{2C}$ receptor involvement in the effects of psilocin and NBOH-2C-CN on 5-HT$_{2A}$ neurons

To examine the role of 5-HT$_{2C}$ receptors 5-HT$_{2A}$ neuron activity and in the effects of psilocin and NBOH-2C-CN, we performed current-clamp recordings with the 5-HT$_{2C}$-specific antagonist RS102221. RS102221 (5 μM) decreased firing in 5-HT$_{2A}$ neurons (n = 11 cells/N = 6 mice, *paired* t-test **p < 0.01; Fig. 5A, B) to ~30% of baseline (n = 11 cells/N = 6 mice, one-sample t-test ****p < 0.0001; Fig. 5C). Subsequent psilocin (10 μM) application with RS102221 (5 μM) increased 5-HT$_{2A}$ neuron firing (n = 11 cells/N = 6 mice, *paired* t-test *p < 0.05; Fig. 5A, D) to ~200% of baseline (n = 10 cells/N = 6 mice, one-sample t-test *p < 0.05; Fig. 5E). In separate recordings, RS102221 (5μM) decreased firing (n = 9 cells/N = 5 mice, *paired* t-test **p < 0.01; Fig. 5F, G) to ~35% of baseline (n = 9 cells/N = 5 mice, one-sample t-test ***p < 0.001; Fig. 5H). Subsequent NBOH-2C-

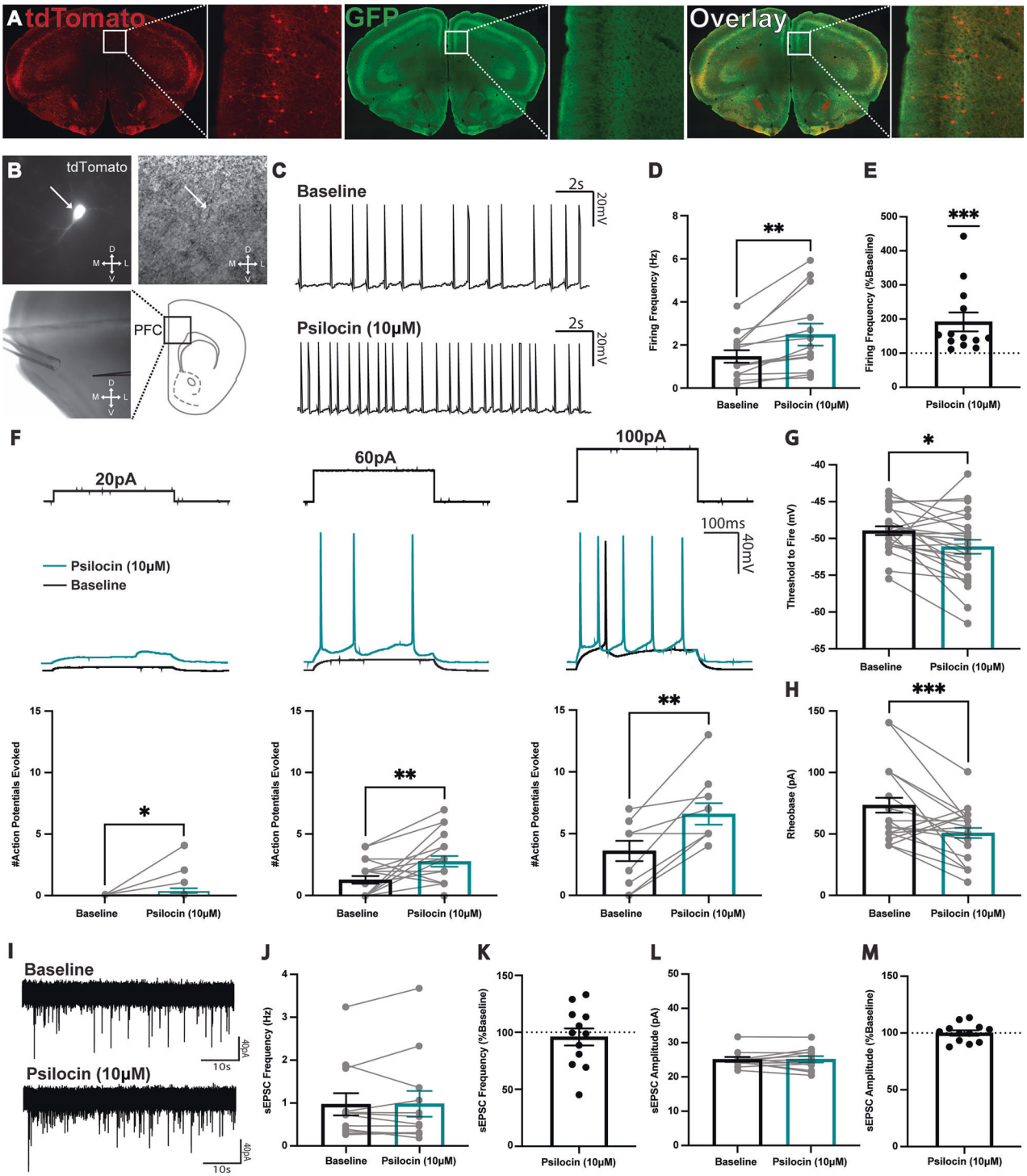

Fig. 2 Psilocin effects on excitability and synaptic transmission in 5-HT2A neurons in medial prefrontal cortex. A Visualization of tamoxifen-induced expression (red) and 5-HT_{2A}R (green) in the PFC of 5-HT_{2A}R-eGFP-CreERT2xAi9 model. **B** Representative 5-HT_{2A} neuron and its location within PFC slice. **C** Representative recording of 5-HT_{2A} neuron firing after psilocin (10 μM). **D** Averaged psilocin effects on firing in 5-HT_{2A} neurons (mean ± SEM, n = 13 cells/N = 10 mice; *paired* t-test **p < 0.01). **E** Normalized psilocin effects on firing in 5-HT_{2A} neurons (mean ± SEM, n = 13 cells/N = 10 mice. One sample t-test ***p < 0.001). **F** Representative recordings of 5-HT_{2A} neuron firing before and after psilocin (10 μM) in response to 400 ms injected currents of 20, 60 and 100 pA with averaged psilocin effect on number of action potentials evoked (mean ± SEM, n = 10–25 cells/N = 12 mice; *paired* t-test *p < 0.05, **p < 0.01, ***p < 0.001). **G** Averaged psilocin effect on threshold to fire (mean ± SEM, n = 25 cells/N = 12 mice; *paired* t-test *p < 0.05). **H** Averaged psilocin effect on rheobase (mean ± SEM, n = 25 cells/N = 12 mice; *paired* t-test ***p < 0.001). **I** Representative recording of 5-HT_{2A} neuron spontaneous excitatory post synaptic currents (sEPSCs) after psilocin (10 μM). **J** Averaged psilocin effect on sEPSC frequency (mean ± SEM, n = 12 cells/N = 8 mice). **K** Normalized psilocin effect on sEPSC frequency (mean ± SEM, n = 12 cells/N = 8 mice). **L** Average of psilocin effect on sEPSC amplitude (mean ± SEM, n = 12 cells/N = 8 mice). **M** Normalized psilocin effect on sEPSC amplitude (mean ± SEM, n = 12 cells/N = 8 mice).

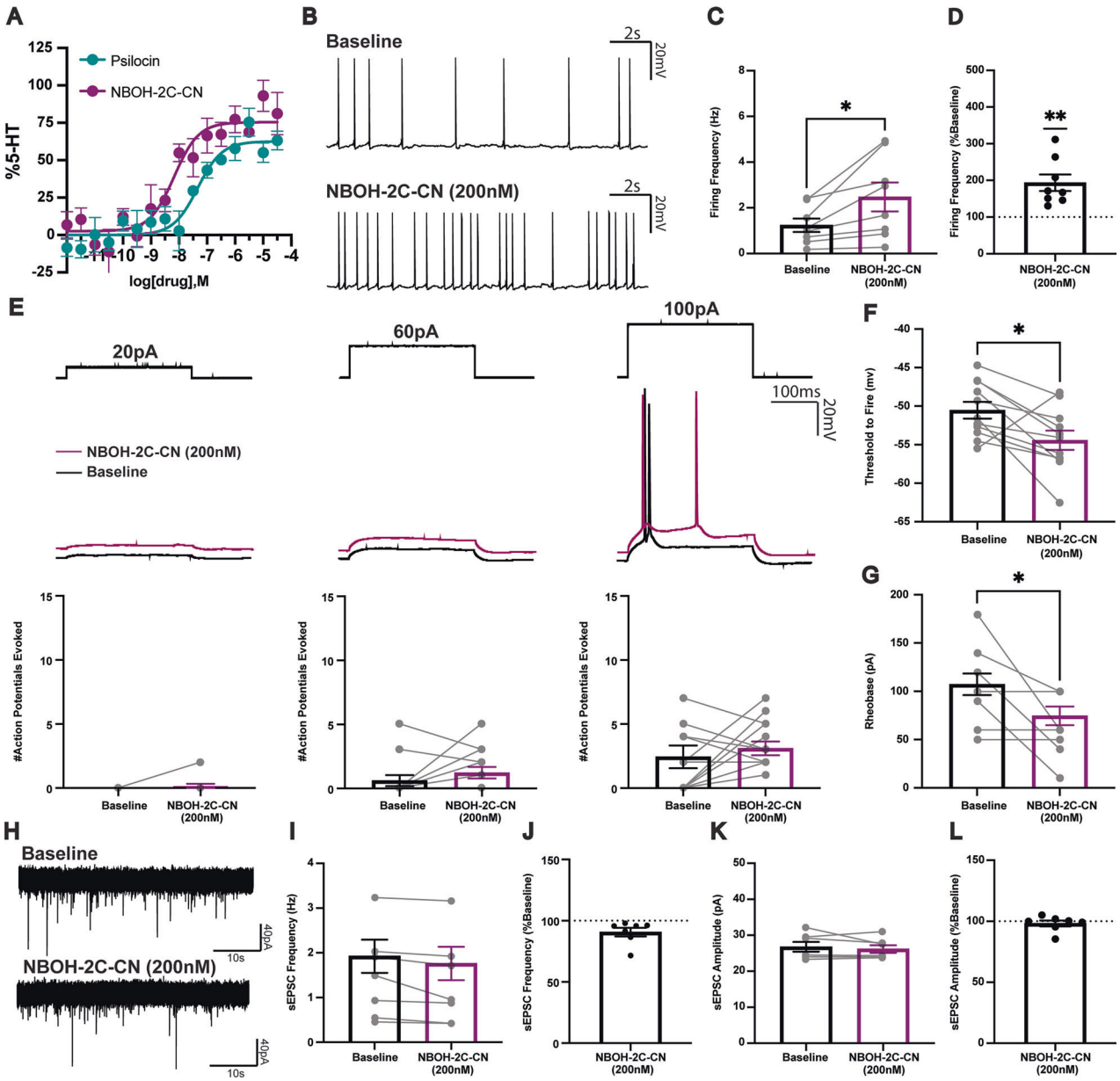

Fig. 3 5-HT2A-selective agonist NBOH-2C-CN effects on excitability and synaptic transmission in 5-HT2A neurons. **A** Gq dissociation concentration-response curves at mouse 5-HT_{2A}R for psychedelic drugs psilocin and NBOH-2C-CN. **B** Representative recording of 5-HT_{2A} neuron firing after NBOH-2C-CN (200 nM). **C** Averaged NBOH-2C-CN effects on firing in 5-HT_{2A} neurons (mean ± SEM, n = 8 cells/N = 4 mice; *paired* t-test *p < 0.05). **D** Normalized NBOH-2C-CN effects on firing in 5-HT_{2A} neurons (mean ± SEM, n = 8 cells/N = 4 mice; one sample t-test **p < 0.01). **E** Representative recordings of 5-HT_{2A} neuron firing before and after NBOH-2C-CN (200 nM) in response to 400 ms injected currents of 20 pA, 60 pA, and 100 pA with averaged NBOH-2C-CN effect on number of action potentials evoked (mean ± SEM, n = 10–12 cells/N = 8 mice). **F** Averaged NBOH-2C-CN effect on threshold to fire (mean ± SEM, n = 11 cells/N = 7 mice; *paired* t-test *p < 0.05). **G** Averaged NBOH-2C-CN effect on rheobase (mean ± SEM, n = 11 cells/N = 7 mice; *paired* t-test *p < 0.05). **H** Representative recording of 5-HT_{2A} sEPSCs after NBOH-2C-CN (200 nM). **I** Averaged NBOH-2C-CN effect on sEPSC frequency (mean ± SEM, n = 7 cells/N = 5 mice). **J** Normalized NBOH-2C-CN effect on sEPSC frequency (mean ± SEM, n = 7 cells/N = 5 mice). **K** Averaged NBOH-2C-CN effect on sEPSC amplitude (mean ± SEM, n = 7 cells/N = 5 mice). **L** Normalized NBOH-2C-CN effect on sEPSC amplitude (mean ± SEM, n = 7 cells/N = 5 mice).

CN (200 nM) application with RS102221 (5μM) increased 5-HT_{2A} neuron firing (n = 10 cells/N = 5 mice, *paired* t-test **p < 0.01; Fig. 5F, I) to ~200% of baseline (n = 10 cells/N = 5 mice, one-sample t-test *p < 0.05; Fig. 5J).

$G\alpha_q$ signaling in the effects of psilocin and NBOH-2C-CN on 5-HT_{2A} neurons

To examine $G\alpha_q$ signaling in the effects of psilocin and NBOH-2C-CN, we performed current-clamp recordings using the selective $G\alpha_q$ inhibitor FR900359. FR900359 (1μM) (Fig. 6A) decreased 5-HT_{2A} neuron firing (n = 10 cells/N = 4 mice, *paired* t-test **p < 0.01; Fig. 6B, C) to ~40% of baseline (n = 10 cells/N = 4 mice, one-sample t-test **p < 0.01; Fig. 6D). Subsequent psilocin (10 μM) application with FR900359 (1μM) did not change 5-HT_{2A} neuron firing in raw (n = 10 cells/N = 4 mice, Fig. 6B, E) or normalized values (n = 10 cells/N = 4 mice, Fig. 6F). In separate recordings, FR900359 (1μM) decreased 5-HT_{2A} neuron firing (n = 6 cells/N = 3 mice, *paired* t-test **p < 0.01; Fig. 6G, H) to ~40% of baseline (n = 6 cells/N = 3 mice, one-sample t-test **p < 0.01; Fig. 6I). Subsequent NBOH-2C-CN (200 nM) application with

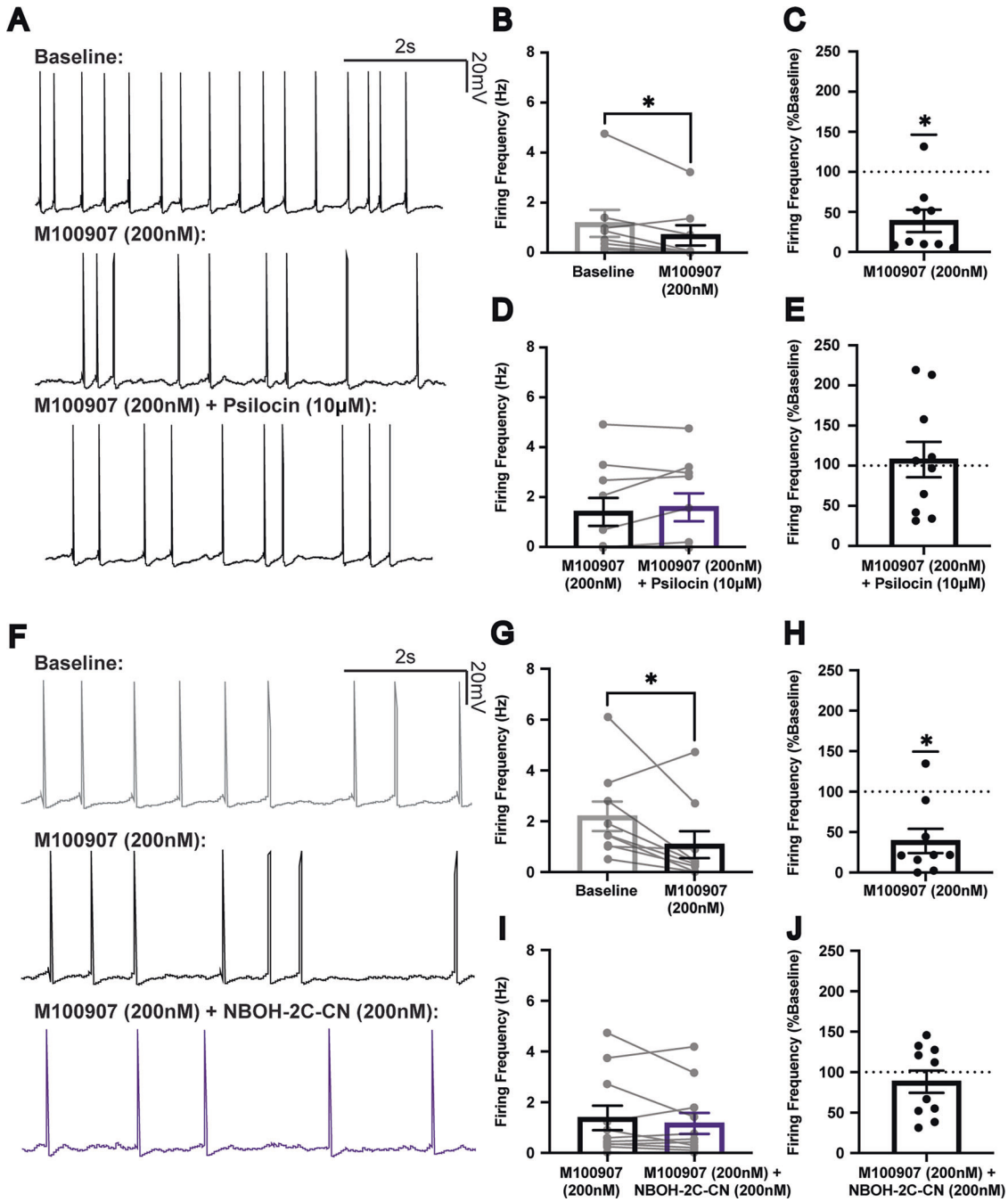

Fig. 4 The role of 5-HT2A receptors in the effects of psilocin and NBOH-2C-CN on 5-HT2A neurons. A Representative recording of 5-HT_{2A} neuron firing after M100907 (200 nM) and psilocin (10 μM). **B** Averaged M100907 effects on firing in 5-HT_{2A} neurons (mean ± SEM, n = 10 cells/N = 6 mice). **C** Normalized M100907 effects on firing in 5-HT_{2A} neurons (mean ± SEM, n = 10 cells/N = 6mice; one sample t-test **p < 0.01). **D** Averaged M100907 + psilocin effects on firing in 5-HT_{2A} neurons (mean ± SEM, n = 10 cells/N = 6 mice). **E** Normalized M100907 + psilocin effects on firing in 5-HT_{2A} neurons (mean ± SEM, n = 10 cells/N = 6 mice). **F** Representative recording of 5-HT_{2A} neuron firing after M100907 (200 nM) and NBOH-2C-CN (200 nM). **G** Averaged M100907 effects on firing in 5-HT_{2A} neurons (mean ± SEM, n = 9 cell/N = 5 mice; *paired* t-test *p < 0.05). **H** Normalized M100907 effects on firing in 5-HT_{2A} neurons (mean ± SEM, n = 9 cells/N = 5 mice; one sample t-test *p < 0.01). **I** Averaged M100907 + NBOH-2C-CN effects on firing in 5-HT_{2A} neurons (mean ± SEM, n = 11 cells/N=5mice). **J** Normalized M100907 + NBOH-2C-CN effects on firing in 5-HT_{2A} neurons (mean ± SEM, n = 10/N = 5 mice).

FR900359 (1μM) did not change 5-HT_{2A} firing in raw (n = 7 cells/N = 3 mice, Fig. 6G, J) or normalized values (n = 7 cells/N = 3 mice, Fig. 6K).

We performed recordings with FR900359 (1 μM) included in the internal pipette solution (Fig. 6L). Psilocin (10μM) with intracellular FR900359 paradoxically decreased firing in 5-HT_{2A} neurons (n = 9 cells/N = 5 mice, *paired* t-test *p < 0.05; Fig. 6M, N), with no significant changes observed in normalized firing (n = 9 cells/N = 5 mice, Fig. 6O). NBOH-2C-CN (200 nM) application with intracellular FR900359 also did not significantly change 5-HT_{2A} neuron firing in raw (n = 8 cells/N = 4 mice, Fig. 6P, Q) or normalized values (n = 8 cells/N = 4 mice, Fig. 6R).

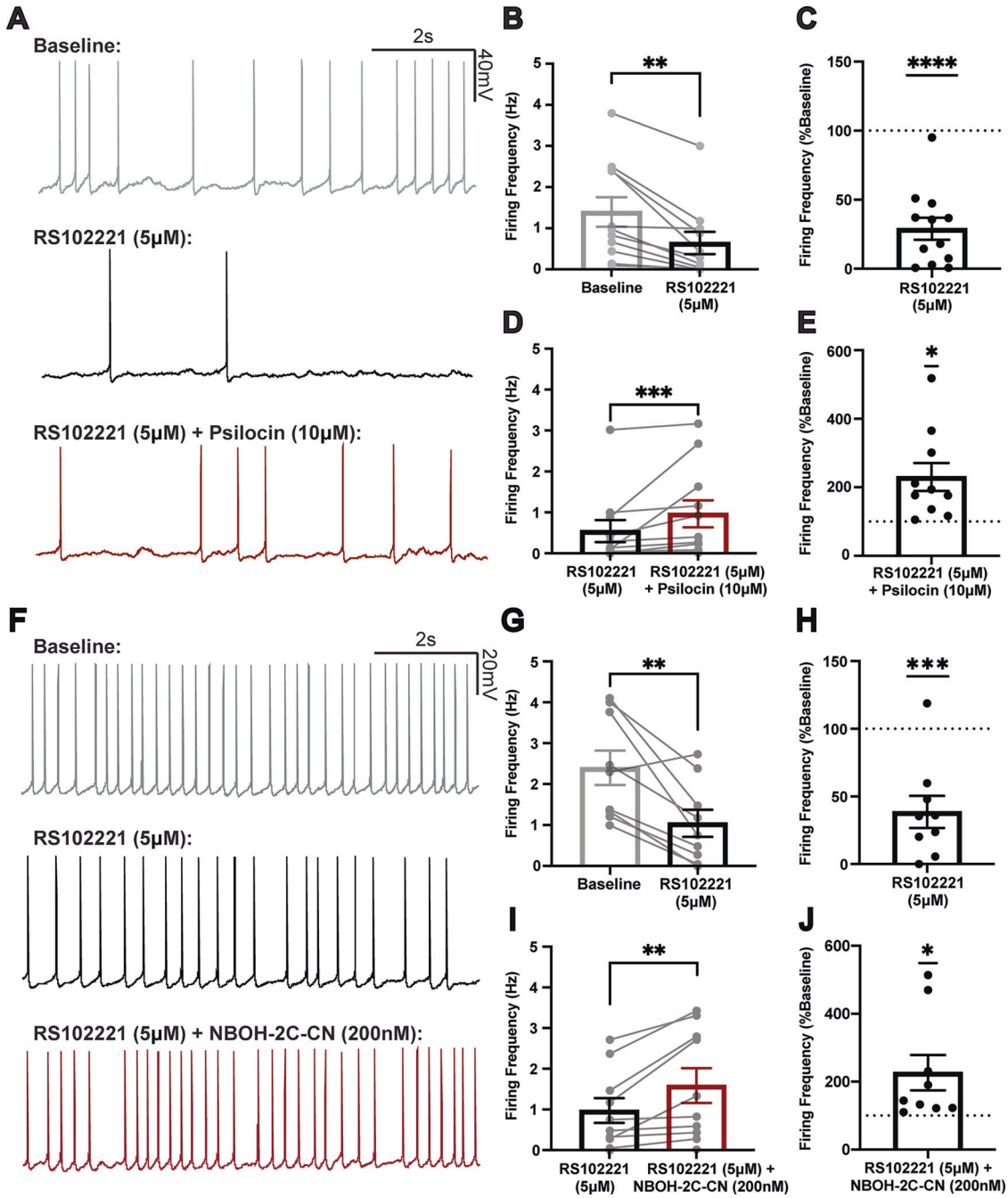

Fig. 5 The role of 5-HT2C receptors in the effects of psilocin and NBOH-2C-CN on 5-HT2A neurons. A Representative recording of 5-HT_{2A} neuron firing after RS102221 (5 μM) and psilocin (10 μM). **B** Averaged RS102221 effects on firing in 5-HT_{2A} neurons (mean ± SEM, n = 11 cells/N = 6 mice; *paired* t-test **p < 0.005). **C** Normalized RS102221 effects on firing in 5-HT_{2A} neurons (mean ± SEM, n = 11 cells/N = 6 mice; one sample t-test ****p < 0.0001). **D** Averaged RS102221 + psilocin effects on firing in 5-HT_{2A} neurons (mean ± SEM, n = 11 cells/N = 6 mice; *paired* t-test *p < 0.05). **E** Normalized RS102221 + psilocin effects on firing in 5-HT_{2A} neurons (mean ± SEM, n = 10 cells/N = 6 mice ; one sample t-test *p < 0.05). **F** Representative recording of 5-HT_{2A} neuron firing after RS102221 (5 μM) and NBOH-2C-CN (200 nM). **G** Averaged RS102221 effects on firing in 5-HT_{2A} neurons (mean ± SEM, n = 9 cells/N = 5 mice; *paired* t-test **p < 0.01). **H** Normalized RS102221 effects on firing in 5-HT_{2A} neurons (mean ± SEM, n = 9 cells/N = 5 mice; one sample t-test ***p < 0.001). **I** Averaged RS102221 + NBOH-2C-CN effects on firing in 5-HT_{2A} neurons (mean ± SEM, n = 10 cells/N = 5 mice; *paired* t-test **p < 0.01). **J** Normalized RS102221 + NBOH-2C-CN effects on firing in 5-HT_{2A} neurons (mean ± SEM, n = 10 cells/N = 5 mice; one sample t-test *p < 0.05).

DISCUSSION

The present study investigated population-specific effects of psilocin in defined regions and populations of mouse medial prefrontal cortex (mPFC). Systemic psilocin increased mPFC activity, specifically in prelimbic (PrL) mPFC. Psilocin produced variable neuronal firing responses, suggesting divergent population-specific effects within PrL/ACC mPFC. Using transgenic 5-HT_{2A} mice, we found that psilocin consistently increased firing in 5-HT_{2A} pyramidal neurons as did the 5-HT_{2A}-selective agonist 25-CN-NBOH. The increased firing with psilocin or 25-CN-NBOH occurred in the absence of changes in excitatory or inhibitory transmission, suggesting direct postsynaptic actions on 5-HT_{2A} neurons and not changes in network activity. The

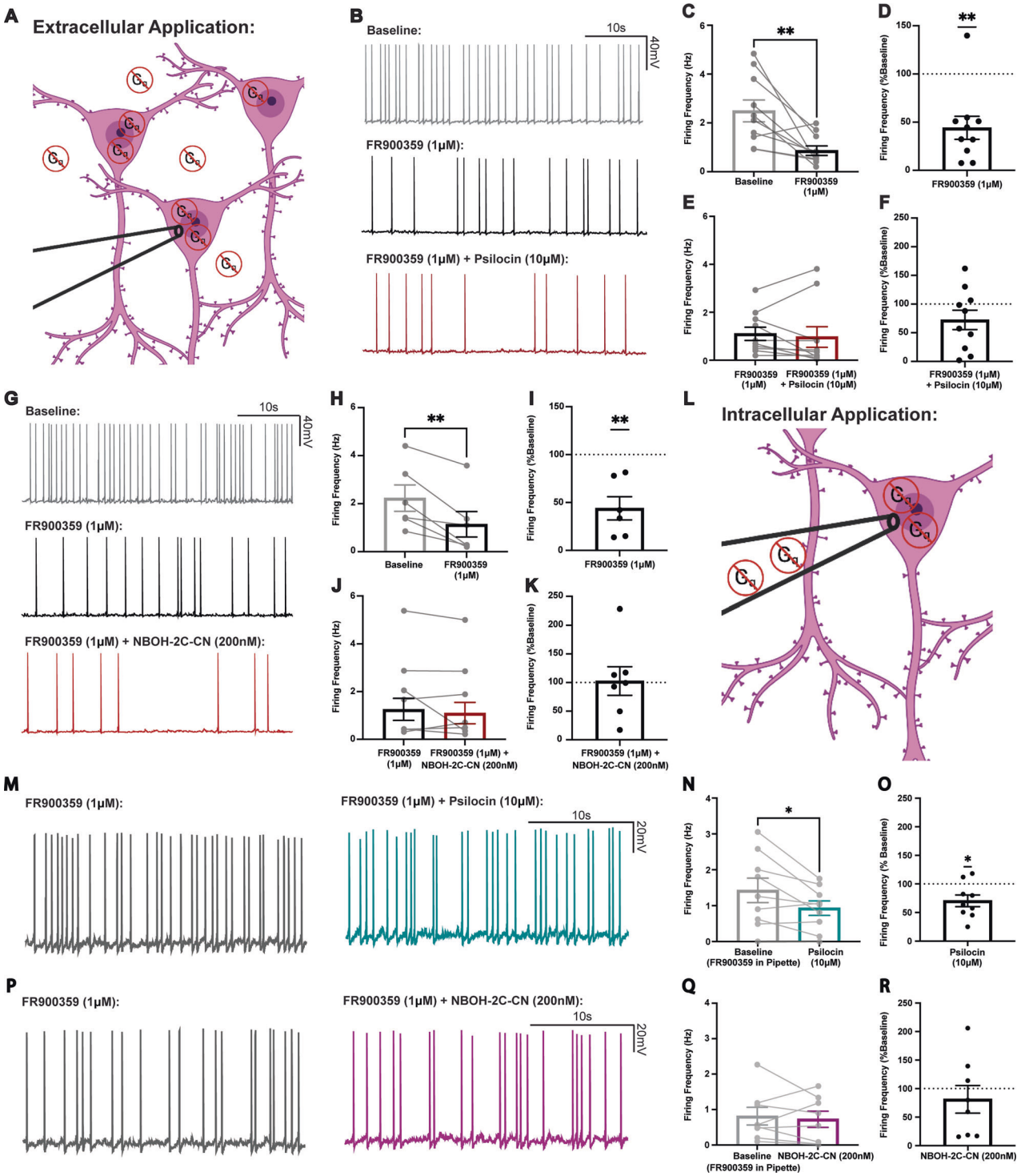

excitatory effects were mediated by 5-HT_{2A} as 5-HT_{2A} (but not 5-HT_{2C}) blockade prevented increased firing with psilocin or 25-CN-NBOH. The increased firing was mediated by $G\alpha_q$ signaling, as global and targeted application of a $G\alpha_q$ inhibitor prevented increased firing with psilocin or 25-CN-NBOH. Collectively, these data illustrate population-specific effects of psychedelics in the mPFC, specifically implicating 5-HT_{2A} neuronal populations in excitatory effects of psychedelic drug administration. These findings provide mechanistic insight into psychedelic drug effects in a brain region implicated in mediating potential therapeutic actions that can guide the rational design of novel antidepressant drugs.

Previous studies indicate that 5-HT_{2A} activation in layer V pyramidal neurons increases glutamatergic signaling [45, 46] depolarization [47] and firing [48]. However, reports of direct excitation with 5-HT_{2A} activation are rare, and some speculate that 5-HT_{2A} activation triggers the release of glutamate from thalamo-cortical fibers via retrograde messenger. We found that psilocin exerted differential effects on firing in unspecified layer V pyramidal neurons. This is consistent with prior studies showing increased firing in only a subset of pyramidal neurons in vivo and ex vivo, suggesting that psychedelics exert differential effects across cortical regions depending on drug, dose, and 5-HT_{2A}

Fig. 6 The role of Gαq signaling in the effects of psilocin and NBOH-2C-CN on 5-HT2A neurons. **A** Cartoon depicting extracellular application of FR900359 drug onto recorded neurons. **B** Representative recording of 5-HT_{2A} neuron firing after FR900359 (1 μM) and psilocin (10 μM). **C** Averaged FR900359 effects on firing in 5-HT_{2A} neurons (mean ± SEM, n = 10 cells/N = 4 mice; *paired* t-test **p < 0.01). **D** Normalized FR900359 effects on firing in 5-HT_{2A} neurons (mean ± SEM, n = 10 cells/N = 4 mice; one sample t-test **p < 0.01). **E** Averaged FR900359 + psilocin effects on firing in 5-HT_{2A} neurons (mean ± SEM, n = 10 cells/N = 4 mice). **F** Normalized FR900359 + psilocin effects on firing in 5-HT_{2A} neurons (mean ± SEM, n = 10 cells/N = 4 mice). **G** Representative recording of 5-HT_{2A} neuron firing after FR900359 (1 μM) and NBOH-2C-CN (200 nM). **H** Averaged FR900359 effects on firing in 5-HT_{2A} neurons (mean ± SEM, n = 6 cells/N = 3 mice; *paired* t-test **p < 0.01). **I** Normalized FR900359 effects on firing in 5-HT_{2A} neurons (mean ± SEM, n = 6 cells/N = 3 mice; one sample t-test **p < 0.01). **J** Averaged FR900359 + NBOH-2C-CN effects on firing in 5-HT_{2A} neurons (mean ± SEM, n = 7 cells/N = 3 mice). **K** Normalized FR900359 + NBOH-2C-CN effects on firing in 5-HT_{2A} neurons (mean ± SEM, n = 7 cells/N = 3 mice). **L** Cartoon depicting intracellular application of FR900359 drug onto recorded neurons. **M** Representative recording of 5-HT_{2A} neuron firing with FR900359 (1 μM) in internal solution and psilocin (10 μM). **N** Averaged FR900359 + psilocin effects on firing in 5-HT_{2A} neurons (mean ± SEM, n = 9 cells/N = 5 mice; *paired* t-test *p < 0.05). **O** Normalized FR900359 + psilocin effects on firing in 5-HT_{2A} neurons (mean ± SEM, n = 9 cells/N = 5 mice). **P** Representative recording of 5-HT_{2A} neuron firing with FR900359 (1 μM) in internal solution and NBOH-2C-CN (200 nM). **Q** Averaged FR900359 + NBOH-2C-CN effects on firing in 5-HT_{2A} neurons (mean ± SEM, n = 8 cells/N = 4 mice.). **R** Normalized FR900359 + NBOH-2C-CN effects on firing in 5-HT_{2A} neurons (mean ± SEM, n = 8 cells/N = 4 mice).

density [49–51]. Importantly, these prior studies did not examine 5-HT_{2A} neurons and only examined unspecified pyramidal neurons. A more recent study found that while increased spine density following psilocybin was observed in both intratelencephalic and pyramidal tract mPFC cells, increases in excitability and reductions in stress-related behaviors were mediated primarily by pyramidal tract cells, and both structural plasticity as well as behavioral changes were abolished in cell-type-targeted 5-HT_{2A} receptor knockout mice [30]. We specifically targeted 5-HT_{2A} neurons and found that psilocin and 25-CN-NBOH significantly increased firing in 5-HT_{2A} neurons. However, in contrast to psilocin, 25-CN-NBOH did not significantly increase the number of action potentials elicited at depolarizing current injections, despite significantly reducing the threshold to fire and rheobase. It is possible that 25-CN-NBOH only increases excitability at lower but not at higher stimulation, or it is also possible that the episodic recording parameters were not sufficient to detect increased firing that was more evident in stable continuous recordings. Overall, these results suggest that 5-HT_{2A} neurons may be uniquely sensitive to the actions of psychedelics and could be the source of increased excitation in the mPFC

We found that psilocin and 25-CN-NBOH increased firing without altering excitatory or inhibitory synaptic transmission in 5-HT_{2A} neurons. While we cannot rule out the possibility of network changes that we were unable to detect, these findings suggest that psilocin increases firing in 5-HT_{2A} PrL/ACC through direct actions and not changes in intrinsic or extrinsic synaptic transmission. The direct excitation of 5-HT_{2A} layer V pyramidal neurons potentially causes an increase in glutamatergic recurrent network activity. Previous work demonstrated that inhibition of post-synaptic 5-HT_{2A} in transfected neurons failed to inhibit increases in sEPSCs [52], which is inconsistent with postsynaptic 5-HT_{2A}-triggered release of a retrograde messenger. We provide evidence for the simpler explanation that 5-HT_{2A} neurons are a discrete mPFC subpopulation capable of increasing glutamatergic signaling in nearby non-5-HT_{2A} neurons.

5-HT_{2A} agonism mediates the psychoactive effects of psychedelics in preclinical models, and human imaging studies have identified the PFC as a key brain region in the effects of psychedelics. Human positron emission tomography (PET) studies demonstrate that psilocin's psychedelic effects are correlated with PFC 5-HT_{2A} occupancy [28]. Additionally, an fMRI study found that the increase in PFC activity one day post-psilocin administration was predictive of treatment response at 5wks post-treatment [53]. One limitation of our study is the relatively low sample size in the fMRI experiments, which may contribute to variability in the observed effects. To address this, we incorporated a control group to account for non-drug related signal fluctuations and employed a linear mixed-effects model to improve statistical rigor. While these measures enhance the reliability of our findings, future studies with larger cohorts will be necessary to further validate and generalize our results. Recent animal studies have questioned the role of 5-HT_{2A} in the antidepressant activity of psychedelics showing that ketanserin, a nonselective 5-HT_2R antagonist, failed to block psilocybin-induced changes in hippocampal synaptic response [54]. We demonstrate that 5-HT_{2A} is required for increased firing in 5-HT_{2A} mPFC neurons as a 5-HT_{2A} antagonist blocked the effects of psilocin and 25-CN-NBOH, suggesting that effects of psilocin across different brain regions may be modulated by different receptors. Future studies will investigate the role of 5-HT_{2A} neurons in different brain regions on behaviors implicated in psychedelic drug actions, including anxiety-like and motivated behaviors.

Currently-available psychedelic compounds including psilocin, 25-CN-NBOH, LSD, and mescaline activate several biogenic amine receptors present in the mPFC in addition to 5-HT_{2A}. One such target is 5-HT_{2C}, with one study showing that 5-HT_{2C} deletion attenuated DOI-induced head twitch response, a measure of purported hallucinogenic-like effects [55]. We found that 5-HT_{2C} antagonism did not prevent increased firing in 5-HT_{2A} neurons with psilocin or 25-CN-NBOH, suggesting that 5-HT_{2C} does not mediate the effects of either compound. Interestingly, we observed a reduction in firing with 5-HT_{2A} or 5-HT_{2C} antagonism, suggesting 5-HT_{2A} and 5-HT_{2C} are both involved in maintaining tonic basal activity; however, only 5-HT_{2A} mediated the direct excitatory effects of psilocin and 25-CN-NBOH on 5-HT_{2A} neurons.

Biased signaling is a phenomenon where certain ligands preferentially activate one signaling pathway. Canonically, GPCRs signal directly through both G protein- and βArr-mediated pathways. It has been proposed that biased ligands may be useful for activating desired (i.e. therapeutically efficacious) pathways rather than undesired (i.e. unwanted side effect-producing) pathways [56]. Whether the hallucinogenic and therapeutic effects of psychedelics are dissociable is an area of growing interest, particularly in novel compound development [25–27]. We tested one novel compound, the $G\alpha_q$-biased R-70 and found that it elicited similar effects to psilocin and NBOH-2C-CN, that were also blocked by 5-HT_{2A} antagonism. This is especially interesting because R-70 exhibits therapeutic effects but is devoid of hallucinogenic actions in rodents [25]. LSD preferentially signals through βArr2 at the 5-HT_{2A} receptor [11, 57] and LSD-elicited responses are significantly attenuated or absent in βArr2-KO mice [58]. We found that the 5-HT_{2A}-mediated effects of psilocin in 5-HT_{2A} neurons are dependent upon a $G\alpha_q$ signaling pathway as inhibition of $G\alpha_q$ signaling in the bath or in the recorded neuron prevented increased firing with psilocin or 25-CN-NBOH. Although there have been reports that psychedelics differentially couple 5-HT_{2A} to Gαi/o signaling in brain [14, 59], our results are consistent with work showing that 5-HT_{2A} mainly couples to Gαq-like transducers [57, 60–63],

and that genetic deletion of one copy of $G\alpha_q$ abolished psychedelic drug-induced c-Fos expression [60].

Understanding region-specific activity is important in the context of psilocin's emerging therapeutic utility. Psychoaffective disorders including anxiety, depression, and substance use are associated with dysregulated activity in the frontal cortex [64] followed by reductions in frontal cortex synapses [65]. Increasing the activity level of specific mPFC neurons may counteract such deficits, providing a mechanism for reducing depressive symptoms and opposing the loss of neural connectivity with advanced disease phenotypes. One study observed increased dendritic spine growth in the frontal cortex of mice 24 h after a single dose of psilocybin with effects persisting up to 28 days [29]. This study provides a potential source of these structural changes in the mPFC occurring after systemic exposure as acute increases in 5-HT_{2A} neuron activity provides one potential mechanism from which these structural changes might originate.

Preclinical studies provide the opportunity for more detailed mechanistic assessments of psychedelic drug action; however, rodent models differ from human experience. While disease states and affective components of psychedelics are difficult to mimic in rodents, preclinical models can directly assess functional consequences of psychedelic drug exposure and underlying mechanisms. We investigated the effects of the classical psychedelic psilocin on 5-HT_{2A} mPFC neurons with a focus on 5-HT_{2A} and 5-HT_{2C}. Given that receptor pharmacology varies among different psychedelic drugs, future studies should examine the effects of other psychedelics as well as non-psychedelic 5-HT_{2A} agonists. The effects of psychedelic drugs have been shown to be altered in naturally-occurring single nucleotide polymorphisms in the 5-HT_{2A} gene [66]. Notably, although mouse and human 5-HT_{2A} sequences are highly conserved, there are potentially functionally relevant differences [67] that could impact drug effects and should also be examined. Mapping circuit-specific sequelae of psilocin-induced changes in 5-HT_{2A} neuron activity will also be important. Our work suggests that psychedelic-induced changes in activity are complex and may involve differential downstream network effects, so future work should also measure changes in other 5-HT_{2A} neuronal populations. One study found that μ-opioid receptor activation blocked excitatory effects of 5-HT_{2A} agonists on layer V pyramidal neurons [68], presumably including 5-HT_{2A} neurons, suggesting that other neuromodulatory systems may be involved in psychedelic drug actions. A clear, detailed understanding of how psychedelics exert their effects is essential for the continued development of any clinical applications. The current study dissects the effects of psilocin in the mPFC as a brain region highly relevant to human disease, and identifies population-specific, 5-HT_{2A}-mediated effects. These findings provide valuable mechanistic insight into the effects of psilocin that may underlie potential therapeutic applications and that can guide the rational design of novel antidepressant drugs.

DATA AVAILABILITY

All data required for evaluation, interpretation and analysis of the conclusions are present in the manuscript and/or the Supplementary Materials. Additional data will be made available by the authors upon request.

REFERENCES

1. Nichols DE. Psychedelics. Pharmacol Rev. 2016;68:264–355. https://doi.org/10.1124/pr.115.011478
2. Slocum ST, Diberto JF, Roth BL. Molecular insights into psychedelic drug action. J Neurochemistry. 2021. https://doi.org/10.1111/jnc.15540
3. Nutt D, Erritzoe D, Carhart-Harris R. Psychedelic psychiatry's brave new world. Cell. 2020;181:24–28. https://doi.org/10.1016/j.cell.2020.03.020
4. Ross S, Bossis A, Guss J, Agin-Liebes G, Malone T, Cohen B, et al. Rapid and sustained symptom reduction following psilocybin treatment for anxiety and depression in patients with life-threatening cancer: a randomized controlled trial. J Psychopharmacol. 2016;30:1165–80. https://doi.org/10.1177/0269881116675512
5. Carhart-Harris RL, Bolstridge M, Day CMJ, Rucker J, Watts R, Erritzoe DE, et al. Psilocybin with psychological support for treatment-resistant depression: six-month follow-up. Psychopharmacology. 2018;235:399–408. https://doi.org/10.1007/s00213-017-4771-x
6. Carhart-Harris R, Giribaldi B, Watts R, Baker-Jones M, Murphy-Beiner A, Murphy R, et al. Trial of psilocybin versus escitalopram for depression. N Engl J Med. 2021;384:1402–11. https://doi.org/10.1056/nejmoa2032994
7. Griffiths RR, Johnson MW, Carducci MA, Umbricht A, Richards WA, Richards BD, et al. Psilocybin produces substantial and sustained decreases in depression and anxiety in patients with life-threatening cancer: a randomized double-blind trial. J Psychopharmacol. 2016;30:1181–97. https://doi.org/10.1177/0269881116675513
8. Wacker D, Wang C, Katritch V, Han GW, Huang X, Vardy E, et al. Structural features for functional selectivity at serotonin receptors. Science. 2013;340:615–9. https://doi.org/10.1126/science.1232808
9. Wang C, Jiang Y, Ma J, Wu H, Wacker D, Katritch V, et al. Structural basis for molecular recognition at serotonin receptors. Science. 2013;340:610–4. https://doi.org/10.1126/science.1232807
10. Rickli A, Moning OD, Hoener MC, Liechti ME. Receptor interaction profiles of novel psychoactive tryptamines compared with classic hallucinogens. Eur Neuropsychopharmacol. 2016;26:1327–37. https://doi.org/10.1016/j.euroneuro.2016.05.001
11. Wacker D, Wang S, McCorvy JD, Betz RM, Venkatakrishnan AJ, Levit A, et al. Crystal structure of an LSD-bound human serotonin receptor. Cell. 2017;168:377–89.e312. https://doi.org/10.1016/j.cell.2016.12.033
12. Peng Y, McCorvy JD, Harpsoe K, Lansu K, Yuan S, Popov P, et al. 5-HT2C receptor structures reveal the structural basis of gpcr polypharmacology. Cell. 2018;172:719–30.e714. https://doi.org/10.1016/j.cell.2018.01.001
13. Glennon RA, Titeler M, McKenney JD. Evidence for 5-HT2 involvement in the mechanism of action of hallucinogenic agents. Life Sci. 1984;35:2505–11. https://doi.org/10.1016/0024-3205(84)90436-3
14. González-Maeso J, Weisstaub NV, Zhou M, Chan P, Ivic L, Ang R, et al. Hallucinogens recruit specific cortical 5-ht2a receptor-mediated signaling pathways to affect behavior. Neuron. 2007;53:439–52. https://doi.org/10.1016/j.neuron.2007.01.008
15. Keiser MJ, Setola V, Irwin JJ, Laggner C, Abbas AI, Hufeisen SJ, et al. Predicting new molecular targets for known drugs. Nature. 2009;462:175–81. https://doi.org/10.1038/nature08506
16. Vollenweider FX, Vollenweider-Scherpenhuyzen MF, Bäbler A, Vogel H, Hell D. Psilocybin induces schizophrenia-like psychosis in humans via a serotonin-2 agonist action. Neuroreport. 1998;9:3897–902. https://doi.org/10.1097/00001756-199812010-00024
17. Kometer M, Schmidt A, Jancke L, Vollenweider FX. Activation of serotonin 2A receptors underlies the psilocybin-induced effects on oscillations, N170 visual-evoked potentials, and visual hallucinations. J Neurosci. 2013;33:10544–51. https://doi.org/10.1523/jneurosci.3007-12.2013
18. Preller KH, Burt JB, Ji JL, Schleifer CH, Adkinson BD, Stampfli P, et al. Changes in global and thalamic brain connectivity in LSD-induced altered states of consciousness are attributable to the 5-HT2A receptor. eLife. 2018;7:e35082 https://doi.org/10.7554/elife.35082
19. Holze F, Vizeli P, Ley L, Muller F, Dolder P, Stocker M, et al. Acute dose-dependent effects of lysergic acid diethylamide in a double-blind placebo-controlled study in healthy subjects. Neuropsychopharmacology. 2021;46:537–44. https://doi.org/10.1038/s41386-020-00883-6
20. Roth BL, Nakaki T, Chuang DM, Costa E. Aortic recognition sites for serotonin (5HT) are coupled to phospholipase C and modulate phosphatidylinositol turnover. Neuropharmacology. 1984;23:1223–5. https://doi.org/10.1016/0028-3908(84)90244-2
21. Roth BL, Willins DL, Kristiansen K, Kroeze WK. 5-Hydroxytryptamine2-family receptors (5-hydroxytryptamine2A, 5-hydroxytryptamine2B, 5-hydroxytryptamine2C): where structure meets function. Pharmacol Ther. 1998;79:231–57. https://doi.org/10.1016/s0163-7258(98)00019-9
22. Gray JA, Bhatnagar A, Gurevich VV, Roth BL. The interaction of a constitutively active arrestin with the arrestin-insensitive 5-ht2areceptor induces agonist-independent internalization. Mol Pharmacol. 2003;63:961–72. https://doi.org/10.1124/mol.63.5.961
23. Gelber EI, Kroeze WK, Willins DL, Gray JA, Sinar CA, Hyde EG, et al. Structure and function of the third intracellular loop of the 5-hydroxytryptamine2A receptor: the third intracellular loop is alpha-helical and binds purified arrestins. J Neurochem. 1999;72:2206–14. https://doi.org/10.1046/j.1471-4159.1999.0722206.x
24. Dong C, Ly C, Dunlap LE, Vargas MV, Sun J, Hwang I, et al. Psychedelic-inspired drug discovery using an engineered biosensor. Cell. 2021;184:2779–92.e2718. https://doi.org/10.1016/j.cell.2021.03.043

25. Kaplan AL, Confair DN, Kim K, Barros-Alvarez X, Rodriguiz RM, Yang Y, et al. Bespoke library docking for 5-HT(2A) receptor agonists with antidepressant activity. Nature. 2022;610:582–91. https://doi.org/10.1038/s41586-022-05258-z
26. Cameron LP, Tombari RJ, Lu J, Pell AJ, Hurley ZQ, Ehinger Y, et al. A non-hallucinogenic psychedelic analogue with therapeutic potential. Nature. 2021;589:474–9. https://doi.org/10.1038/s41586-020-3008-z
27. Cao D, Yu J, Wang H, Luo Z, Liu X, He L, et al. Structure-based discovery of nonhallucinogenic psychedelic analogs. Science. 2022;375:403–11. https://doi.org/10.1126/science.abl8615
28. Madsen MK, Fisher PM, Burmester D, Dyssegaard A, Stenbaek DS, Kristiansen S, et al. Psychedelic effects of psilocybin correlate with serotonin 2A receptor occupancy and plasma psilocin levels. Neuropsychopharmacology. 2019;44:1328–34. https://doi.org/10.1038/s41386-019-0324-9
29. Shao LX, Liao C, Gregg I, Davoudian PA, Savalia NK, Delagarza K, et al. Psilocybin induces rapid and persistent growth of dendritic spines in frontal cortex in vivo. Neuron. 2021;109:2535–44.e2534. https://doi.org/10.1016/j.neuron.2021.06.008
30. Shao LX, Liao C, Davoudian PA, Savalia NK, Jiang Q, Wojtasiewicz C, et al. Psilocybin's lasting action requires pyramidal cell types and 5-HT(2A) receptors. Nature. 2025;642:411–20. https://doi.org/10.1038/s41586-025-08813-6
31. Johnson MW, Garcia-Romeu A, Griffiths RR. Long-term follow-up of psilocybin-facilitated smoking cessation. Am J Drug Alcohol Abuse. 2017;43:55–60. https://doi.org/10.3109/00952990.2016.1170135
32. Davis AK, Barrett FS, May DG, Cosimano MP, Sepeda ND, Johnson MW, et al. Effects of psilocybin-assisted therapy on major depressive disorder: a randomized clinical trial. JAMA Psychiatry. 2021;78:481–89. https://doi.org/10.1001/jamapsychiatry.2020.3285
33. Vollenweider FX, Preller KH. Psychedelic drugs: neurobiology and potential for treatment of psychiatric disorders. Nat Rev Neurosci. 2020;21:611–24. https://doi.org/10.1038/s41583-020-0367-2
34. Hsu L-M, Wang S, Walton L, Wang TW, Lee S-H, Shih YI. 3D U-net improves automatic brain extraction for isotropic rat brain magnetic resonance imaging data. Front Neurosci. 2021;15:801008 https://doi.org/10.3389/fnins.2021.801008
35. Hsu L-M, Wang S, Ranadive P, Ban W, Chao TH, Song S, et al. Automatic skull stripping of rat and mouse brain MRI data using U-net. Front Neurosci. 2020;14:568614 https://doi.org/10.3389/fnins.2020.568614
36. Cox RW. AFNI: software for analysis and visualization of functional magnetic resonance neuroimages. Comput Biomed Res. 1996;29:162–73. https://doi.org/10.1006/cbmr.1996.0014
37. Sunkin SM, Ng L, Lau C, Dolbeare T, Gilbert TL, Thompson CL, et al. Allen Brain Atlas: an integrated spatio-temporal portal for exploring the central nervous system. Nucleic Acids Res. 2013;41:D996–D1008. https://doi.org/10.1093/nar/gks1042
38. Verbeke, G Linear mixed models in practice. in:Lecture notes in statistics Vol. 126 Springer; 1997.
39. Hsu LM, Yang J-T, We X, Liang X, Lin L-C, Huang Y-C, et al. Human thirst behavior requires transformation of sensory inputs by intrinsic brain networks. BMC Biol. 2022;20:255 https://doi.org/10.1186/s12915-022-01446-5
40. Schrage R, Schmitz A-L, Gaffal E, Annala S, Kehraus S, Wenzel D, et al. The experimental power of FR900359 to study Gq-regulated biological processes. Nat Commun. 2015;6:10156 https://doi.org/10.1038/ncomms10156
41. Kenakin T, Watson C, Muniz-Medina V, Christopoulos A, Novick S. A simple method for quantifying functional selectivity and agonist bias. ACS Chem Neurosci. 2012;3:193–203. https://doi.org/10.1021/cn200111m
42. Zhuk O, Jasicka-Misiak I, Poliwoda A, Kazakova A, Godovan VV, Halama M, et al. Research on acute toxicity and the behavioral effects of methanolic extract from psilocybin mushrooms and psilocin in mice. Toxins. 2015;7:1018–29. https://doi.org/10.3390/toxins7041018
43. Halberstadt AL, Koedood L, Powell SB, Geyer MA. Differential contributions of serotonin receptors to the behavioral effects of indoleamine hallucinogens in mice. J Psychopharmacol. 2011;25:1548–61. https://doi.org/10.1177/0269881110388326
44. Olsen RHJ, DiBerto JF, English JG, Glaudin AM, Krumm BE, Slocum ST, et al. TRUPATH, an open-source biosensor platform for interrogating the GPCR transducerome. Nat Chem Biol. 2020;16:841–49. https://doi.org/10.1038/s41589-020-0535-8
45. Aghajanian GK, Marek GJ. Serotonin, via 5-HT2A receptors, increases EPSCs in layer V pyramidal cells of prefrontal cortex by an asynchronous mode of glutamate release. Brain Res. 1999;825:161–71. https://doi.org/10.1016/s0006-8993(99)01224-x
46. Marek GJ. Interactions of hallucinogens with the glutamatergic system: permissive network effects mediated through cortical layer V Pyramidal neurons. Curr Top Behav Neurosci. 2018;36:107–35. https://doi.org/10.1007/7854_2017_480
47. Davies MF, Deisz RA, Prince DA, Peroutka SJ. Two distinct effects of 5-hydroxytryptamine on single cortical neurons. Brain Res. 1987;423:347–52. https://doi.org/10.1016/0006-8993(87)90861-4
48. Araneda R, Andrade R. 5-Hydroxytryptamine2 and 5-hydroxytryptamine 1A receptors mediate opposing responses on membrane excitability in rat association cortex. Neuroscience. 1991;40:399–412. https://doi.org/10.1016/0306-4522(91)90128-b
49. Puig MV, Celada P, Díaz-Mataix L, Artigas F. In vivo modulation of the activity of pyramidal neurons in the rat medial prefrontal cortex by 5-HT2A receptors: relationship to thalamocortical afferents. Cereb Cortex. 2003;13:870–82. https://doi.org/10.1093/cercor/13.8.870
50. Wood J, Kim Y, Moghaddam B. Disruption of prefrontal cortex large scale neuronal activity by different classes of psychotomimetic drugs. J Neurosci. 2012;32:3022–31. https://doi.org/10.1523/jneurosci.6377-11.2012
51. Lladó-Pelfort L, Celada P, Riga MS, Troyano-Rodriguiz E, Santana N, Artigas F. Effects of hallucinogens on neuronal activity. Curr Top Behav Neurosci. 2018;36:75–105. https://doi.org/10.1007/7854_2017_473
52. Béïque JC, Imad M, Mladenovic L, Gingrich JA, Andrade R. Mechanism of the 5-hydroxytryptamine 2A receptor-mediated facilitation of synaptic activity in prefrontal cortex. Proc Natl Acad Sci USA. 2007;104:9870–75. https://doi.org/10.1073/pnas.0700436104
53. Carhart-Harris RL, Roseman L, Bolestridge M, Demetriou L, Nienke Pannekoek J, Wall MB, et al. Psilocybin for treatment-resistant depression: fMRI-measured brain mechanisms. Sci Rep. 2017;7:13187 https://doi.org/10.1038/s41598-017-13282-7
54. Hesselgrave N, Troppoli TA, Wulff AB, Cole AB, Thompson SM. Harnessing psilocybin: antidepressant-like behavioral and synaptic actions of psilocybin are independent of 5-HT2R activation in mice. Proc Natl Acad Sci USA. 2021;118:e2022489118 https://doi.org/10.1073/pnas.2022489118
55. Canal CE, Olaghere da Silva UB, Gresch PJ, Watt EE, Sanders-Bush E, Airey DC. The serotonin 2C receptor potently modulates the head-twitch response in mice induced by a phenethylamine hallucinogen. Psychopharmacology. 2010;209:163–74. https://doi.org/10.1007/s00213-010-1784-0
56. Wacker D, Stevens RC, Roth BL. How ligands illuminate GPCR molecular pharmacology. Cell. 2017;170:414–27. https://doi.org/10.1016/j.cell.2017.07.009
57. Kim K, Che T, Panova O, DiBerto JF, Lyu J, Krumm BE, et al. Structure of a hallucinogen-activated Gq-coupled 5-HT(2A) serotonin receptor. Cell. 2020;182:1574–88.e1519. https://doi.org/10.1016/j.cell.2020.08.024
58. Rodriguiz RM, Nadkarni V, Means CR, Pogorelov VM, Chiu Y-T, Roth BL, et al. LSD-stimulated behaviors in mice require β-arrestin 2 but not β-arrestin 1. Sci Rep. 2021;11:17690 https://doi.org/10.1038/s41598-021-96736-3
59. García-Bea A, Miranda-Azpiazu P, Muguruza C, Marmolejo-Martinez-Artesero S, Diez-Alarcia R, Gabilondo AM, et al. Serotonin 5-HT(2A) receptor expression and functionality in postmortem frontal cortex of subjects with schizophrenia: selective biased agonism via G(αi1)-proteins. Eur Neuropsychopharmacol. 2019;29:1453–63. https://doi.org/10.1016/j.euroneuro.2019.10.013
60. Garcia EE, Smith RL, Sanders-Bush E. Role of G(q) protein in behavioral effects of the hallucinogenic drug 1-(2,5-dimethoxy-4-iodophenyl)-2-aminopropane. Neuropharmacology. 2007;52:1671–77. https://doi.org/10.1016/j.neuropharm.2007.03.013
61. Garnovskaya MN, Nebigil CG, Arthur JM, Spurney RF, Raymond JR. 5-hydroxytryptamine2A receptors expressed in rat renal mesangial cells inhibit cyclic AMP accumulation. Mol Pharmacol. 1995;48:230–7.
62. Goppelt-Struebe M, Stroebel M. Signaling pathways mediating induction of the early response genes prostaglandin G/H synthase-2 and egr-1 by serotonin via 5-HT2A receptors. J Cell Physiol. 1998;175:341–37. 10.1002/(sici)1097-4652(199806)175:3<341::Aid-jcp12>3.0.Co;2-8
63. Saucier C, Albert PR. Identification of an endogenous 5-hydroxytryptamine2A receptor in NIH-3T3 cells: agonist-induced down-regulation involves decreases in receptor RNA and number. J Neurochem. 1997;68:1998–2011. https://doi.org/10.1046/j.1471-4159.1997.68051998.x
64. Pizzagalli DA, Roberts AC. Prefrontal cortex and depression. Neuropsychopharmacology. 2022;47:225–46. https://doi.org/10.1038/s41386-021-01101-7
65. Holmes SE, Scheinost D, Finnema SJ, Naganawa M, Davis MT, DellaGioia N, et al. Lower synaptic density is associated with depression severity and network alterations. Nat Commun. 2019;10:1529 https://doi.org/10.1038/s41467-019-09562-7
66. Schmitz GP, Jain MK, Slocum ST, Roth BL. 5-HT(2A) SNPs alter the pharmacological signaling of potentially therapeutic psychedelics. ACS Chem Neurosci. 2022. https://doi.org/10.1021/acschemneuro.1c00815
67. Dougherty JP, Aloyo VJ. Pharmacological and behavioral characterization of the 5-HT2A receptor in C57BL/6N mice. Psychopharmacology. 2011;215:581–93. https://doi.org/10.1007/s00213-011-2207-6
68. Marek GJ. Behavioral evidence for mu-opioid and 5-HT2A receptor interactions. Eur J Pharmacol. 2003;474:77–83. https://doi.org/10.1016/s0014-2999(03)01971-x

ACKNOWLEDGEMENTS

This work was supported by the Brain and Behavior Research Foundation NARSAD Young Investigator Award (MAH), grants from the National Institutes of Health MH112205 (BLR), DA045657, (BLR), AA011605 (MAH), and AA026858 (MAH), and

funding from the Defense Advanced Research Projects Agency DARPA-5822 HR00112020029 (BLR).

AUTHOR CONTRIBUTIONS

GPS contributed to experimental design, conception, data acquisition, data analysis, visualization, original and revised manuscript drafting, and review/editing; YTC contributed to data acquisition and data analysis, MLF, SM, MM, LMH contributed to experimental design and data acquisition, GMK, EK, YIS contributed to experimental design and key experimental resources, MAH and BLR contributed to conception, experimental design, manuscript drafting, review, and editing, supervision, and funding acquisition.

COMPETING INTERESTS

The authors declare no competing interests.

ADDITIONAL INFORMATION

Supplementary information The online version contains supplementary material available at https://doi.org/10.1038/s41398-025-03611-0.

Correspondence and requests for materials should be addressed to Melissa A. Herman.

Reprints and permission information is available at http://www.nature.com/reprints

Publisher's note Springer Nature remains neutral with regard to jurisdictional claims in published maps and institutional affiliations.

Open Access This article is licensed under a Creative Commons Attribution-NonCommercial-NoDerivatives 4.0 International License, which permits any non-commercial use, sharing, distribution and reproduction in any medium or format, as long as you give appropriate credit to the original author(s) and the source, provide a link to the Creative Commons licence, and indicate if you modified the licensed material. You do not have permission under this licence to share adapted material derived from this article or parts of it. The images or other third party material in this article are included in the article's Creative Commons licence, unless indicated otherwise in a credit line to the material. If material is not included in the article's Creative Commons licence and your intended use is not permitted by statutory regulation or exceeds the permitted use, you will need to obtain permission directly from the copyright holder. To view a copy of this licence, visit http://creativecommons.org/licenses/by-nc-nd/4.0/.

© The Author(s) 2025